Diabetologia (2003) 46:479–491
DOI 10.1007/s00125-003-1073-0

Diabetologia

Insulin signalling pathways in aorta and muscle from two animal models of insulin resistance – the obese middle-aged and the spontaneously hypertensive rats

H. G. Zecchin[1], R. M. N. Bezerra[1], J. B. C. Carvalheira[1], M. A. Carvalho-Filho[1], K. Metze[2], K. G. Franchini[1], M. J. A. Saad[1]

[1] Departamento de Clínica Médica, Faculdade de Ciências Médicas, Universidade Estadual de Campinas, Cidade Universitária, Campinas, São Paulo, Brasil
[2] Departamento de Anatomia Patológica, Faculdade de Ciências Médicas, Universidade Estadual de Campinas, Campinas, Brasil

Abstract

Aims/hypothesis. The aim of this study was to investigate insulin signalling pathways directly in vivo in skeletal muscle and thoracic aorta from obese middle-aged (12-month-old) rats, which have insulin resistance but not cardiovascular disease, and from spontaneously hypertensive rats (SHR), an experimental model of insulin resistance and cardiovascular disease.
Methods. We have used in vivo insulin infusion, followed by tissue extraction, immunoprecipitation and immunoblotting.
Results. Obese middle-aged rats and the SHR showed marked insulin resistance, which parallels the reduced effects of this hormone in the insulin signalling cascade in muscle. In aortae from obese middle-aged rats, the PI 3-kinase/Akt pathway is preserved, leading to a normal activation of endothelial nitric oxide synthase. In SHR this pathway is severely blunted, with reductions in eNOS protein concentration and activation. Both animals, however, showed higher concentrations and higher tyrosine phosphorylation of mitogen-activated protein (MAP) kinase isoforms in aortae.
Conclusions/interpretation. Alterations in the IRS/PI 3-K/Akt pathway in muscle of 12-month-old rats and SHR could be involved in the insulin resistance of these animals. The preservation of this pathway in aorta of 12-month-old rats, apart from increases in MAP kinase protein concentration and activation, could be a factor that contributes to explaining the absence of cardiovascular disease in this animal model. However, in aortae of SHR, the reduced insulin signalling through IRS/PI 3-kinase/Akt/eNOS pathway could contribute to the endothelial dysfunction of this animal. [Diabetologia (2003) 46:479–491]

Keywords Aging, obesity, insulin resistance, aorta, phosphatidylinositol 3-kinase, MAP kinase, Akt, endothelial cell-nitric oxide synthase, SHR.

Received: 15 July 2002 / Revised: 4 December 2002
Published online: 5 April 2003

Corresponding author: M. J. A. Saad, Departamento de Clínica Médica, Faculdade de Ciências Médicas, Universidade Estadual de Campinas, Cidade Universitária, Campinas, São Paulo, 13083-970 Brasil
E-mail: msaad@fcm.unicamp.br
Abbreviations: αPY, Antibody against phosphotyrosine; eNOS, endothelial cell-nitric oxide synthase; ERK, extracellular signal-related kinase; IR, insulin receptor; IRβ, insulin receptor β subunit; IRS, insulin receptor substrate; MAP kinase, mitogen-activated protein kinase; MEK, MAP/ERK kinase; NO, nitric oxide; PAI-1, plasminogen activator inhibitor-1; PI, phosphatidylinositol; PKB, protein kinase B; PMSF, phenylmethylsulfonyl fluoride; SH2, src-homology 2 domain; SH3, src-homology 3 domain; Shc, src-homology 2 domain-containing; SHR, spontaneously hypertensive rats; VSMC, vascular smooth muscle cell.

Introduction

Insulin regulates many vascular functions under physiological conditions. Biological actions of insulin in vascular cells include increases in amino acid transport, glycogen synthesis, DNA synthesis and gene expression [1, 2]. It also has specific vascular actions, such as enhancing the release of nitric oxide (NO) [3], regulating mRNA expression of matrix proteins [4, 5], and constitutive endothelial NO synthase (eNOS) [6, 7]. Physiologically, insulin infusion stimulates local vasodilation by enhancing the action of NO [8, 9].

Normal endothelial production of NO plays an important role in preventing vascular disease. In addition to its function as an endogenous vasodilator, NO released from endothelial cells is a potent inhibitor of

platelet aggregation and adhesion to the vascular wall and also controls the expression of proteins involved in atherogenesis [10].

In vascular cells, insulin actions are initiated through binding to the insulin receptor alfa subunit, which activates the intrinsic receptor tyrosine kinase [11], resulting in autophosphorylation of insulin receptor beta subunit (IRβ) and tyrosine phosphorylation of intracellular adapter proteins such as insulin receptor substrates (IRS-1 and IRS-2) [12, 13] and Shc [14]. Tyrosine-phosporylated IRS-1 or IRS-2 binds to src-homology 2 (SH2) domains of intracellular proteins, including the p85 regulatory subunit of phosphatidylinositol (PI) 3-kinase [15]. The interaction of IRS and p85 subunit of PI 3-kinase results in the activation of p110 catalytic subunit of PI 3-kinase. In the vasculature, the activation of PI 3-kinase increases serine phosphorylation of Akt which, in turn, directly phosphorylates eNOS on serine 1177 and activates the enzyme, leading to increased NO production [16, 17].

It has been proposed that some of the actions of insulin in the vasculature, such as the stimulatory effects on NO production, are selectively inhibited in the obese Zucker rats, which present insulin resistance and hypertension. However, other animal models of insulin resistance have normal blood pressure and no cardiovascular disease.

We have characterized insulin signalling pathways directly in vivo in skeletal muscle and thoracic aortae from two animal models of insulin resistance: the obese middle-aged Wistar rats, which do not present vascular dysfunction, and the spontaneously hypertensive rats (SHR), an animal model of insulin resistance with profound vascular dysfunction on the basis of hypertension in the absence of lipid disorders.

Materials and methods

Experimental animals. Male Wistar rats were obtained from the UNICAMP Central Animal Breeding Center (Campinas, Sao Paulo, Brazil) and divided into two groups by age (2 and 12 months old) with body weights of 137±2.4 and 432.6±2.7 g, respectively. Twenty-week-old male SHR were compared to the age-matched normotensive, insulin-sensitive Wistar-Kyoto (WKY) strain. Animals were allowed free access to standard rodent chow and water ad libitum. Food was withdrawn 12 h before the experiments. All experiments involving animals were approved by the ethics committee at the University of Campinas.

Blood samples were taken for measuring plasma concentration of total cholesterol and triglycerides. Lipids were measured in a routine diagnostic analyser (Modular, Roche Diagnostics) using enzymatic colorimetric assays (cholesterol, CHOD-PAP assay; triglycerides, GPO-PAP assay). Plasma glucose concentrations were measured by the glucose oxidase method, as described previously [18]. Serum insulin was determined by radioimmunoassay [19].

Antibodies and Chemicals. The reagents and apparatus for SDS-PAGE and immunoblotting were obtained from Bio-Rad (Richmond, Calif., USA). TRIS, phenylmethylsulfonylfluoride (PMSF), aprotinin, dithiothreitol, Triton X-100, Tween-20 and glycerol were obtained from Sigma Chemical (St. Louis, Mo., USA). Human recombinant insulin (Humulin R) and sodium amobarbital were purchased from Eli Lilly (Indianapolis, Ind., USA). [^{125}I]Protein A was obtained from Amersham (Aylesbury, UK), and protein A-Sepharose 6 MB was obtained from Pharmacia Biotech (Uppsala, Sweden). Nitrocellulose (BA85; 0.2 μm) was purchased from Schleicher & Schuell, (Keene, N.H., USA). Molecular weight, M_r standards were myosin (194 kDa), β-galactosidade (116 kDa), BSA (85 kDa) and ovalbumin (49.5 kDa).

Monoclonal antiphosphotyrosine (αPY) and anti-PI 3-kinase (p85) antibodies were obtained from Upstate Biotechnology (UBI – Lake Placid, N.Y., USA). Polyclonal antibodies against beta subunit of insulin receptor (C-19, sc-711), IRS-1 (C-20, sc-559), IRS-2 (A-19, sc-1556), eNOS (NOS3, C-20, sc-654), phospho-eNOS (Ser 1177, sc-12972), Akt1 (C-20, sc-1618), Shc (C-20, sc-288: specific for Shc p46, p52 and p66) and ERK1 (C-16, sc-93: reactive with ERK1 p44 and, to a lesser extent, ERK2 p42), as well as the monoclonal antibody against phospho-ERK (Tyr 204, E-4, sc-7383) were purchased from Santa Cruz Biotechnology (Santa Cruz, Calif., USA). Polyclonal antibodies against phospho-Akt (Ser 473) were obtained from New England Biolabs (Beverly, Mass., USA).

Buffers. Buffer A consisted of 100 mmol/l TRIS, 1% sodium dodecyl sulphate (SDS), 50 mmol/l HEPES (pH 7.4), 100 mmol/l sodium pyrophosphate, 100 mmol/l sodium fluoride, 10 mmol/l EDTA and 10 mmol/l sodium vanadate. Buffer B was similar to buffer A except that 1% Triton X-100 replaced 1% SDS and 2 mmol/l phenylmethylsulphonic fluoride (PMSF) and 0.1 mg/ml aprotinin were added. Buffer C contained 100 mmol/l TRIS, 10 mmol/l sodium vanadate, 10 mmol/l EDTA and 1% Triton X-100.

Immunoprecipitation and Western immunoblotting. Rats were anaesthetized by intraperitoneal injection of sodium amobarbital (100 mg/kg body weight) and the experiments were done after the loss of corneal and pedal reflexes. The abdominal cavity was opened, the cava vein was exposed, and 0.5 ml of normal saline (0.9% NaCl) with or without 10^{-5} mol/l of insulin was injected. Thoracic aorta and hind limb skeletal muscle were isolated after 60, 90 or 180 s (according to the protein studied), frozen with liquid N_2, powdered with a glass Dounce homogenizer on ice for at least 80 strokes and immediately homogenized in freshly prepared, boiling buffer A when intended for immunoblots, or freshly prepared, ice-cold buffer B when intended for immunoprecipitation. The extracts were centrifuged at 30 000×g and 4°C in a Beckman Coulter 70.1 Ti rotor (Palo Alto, Calif., USA) for 45 min to remove insoluble material. Protein concentration in the supernatants was determined by the Bradford method [20].

For immunoprecipitations, samples containing 3 mg of total protein were incubated with antibodies against IRβ (0.3 mg/ml), IRS-1 (1:1000 dilution), IRS-2 (1:1000), Shc (1:1000) or eNOS (1:500) at 4°C overnight, followed by the addition of Protein A Sepharose 6 MB for 1 h. The pellets were repeatedly washed in buffer C (five times), resuspended in 50 ml of Laemmli sample buffer [21], and boiled for 5 min before loading onto the gel. For immunoblotting, similar sized aliquots (200 mg of total protein) were suspended in 50 ml of Laemmli sample buffer containing 100 mmol/l dithiothreitol and boiled for 5 min before loading onto a 8% SDS-polyacrylamide gel electrophoresis (SDS-PAGE) system in a miniature slab gel apparatus from Bio-Rad.

Electrotransfer of proteins from the gel to nitrocellulose was carried out for 2 h at 120 V (constant) in a Bio-Rad miniature transfer apparatus (Mini-Protean) as described previously [22] except for adding the 0.02% of SDS to the transfer buffer to enhance the elution of high molecular mass proteins. Non specific protein binding to the nitrocellulose was reduced by preincubating the filter overnight at 4°C in blocking buffer (5% non-fat dry milk, 10 mmol/l TRIS, 150 mmol/l NaCl, and 0.02% Tween-20). The nitrocellulose blot was then incubated with the following antibodies: antiphosphotyrosine (1 mg/ml), anti-p85 subunit of PI 3-kinase (1:500), anti-insulin receptor (1:100), anti-IRS-1 (1:100), anti-IRS-2 (1:100), anti-Shc (1:1000), anti-ERK1/2 (p44/42 MAP kinase, 1:1000), anti-tyrosine-phosphorylated ERK1/2 (1:1000), anti-Akt1 (1:1000), anti-phospho-(ser-473)-Akt (1:1000), anti-eNOS (1:1000) and anti-phospho-(ser-1177)-eNOS (1:1000), each one diluted in blocking buffer (0.3% BSA instead of non-fat dry milk) overnight at 4°C, and then washed for 60 min with blocking buffer without milk. The blots were subsequently incubated with 0.074 MBq [^{125}I]protein A (1.11 MBq/μg) in 10 ml blocking buffer for 2 h at room temperature and then washed again for 30 min as described above. [^{125}I]Protein A bound to the antiphosphotyrosine and antipeptide antibodies was detected by autoradiography using preflashed Kodak XAR film (Eastman Kodak, Rochester, N.Y., USA) with Cronex Lightning Plus intensifying screens (DuPont, Wilmington, Del., USA) at −80°C for 12 to 48 h. Band intensities were quantitated by optical densitometry (model GS 300, Hoefer Scientific Instruments, San Francisco, Calif., USA) of the developed autoradiographs.

Fifteen-minute insulin tolerance test Rats were fasted overnight and submitted to an intravenous insulin tolerance test (IVITT; 1 U/kg body weight of insulin, i.v.) and samples for blood glucose measurements were collected at 0 (basal), 4, 8, 12, and 16 min after injection. Rats were anaesthetized with sodium amobarbital as described above, 40 μl of blood was collected from their tails and blood glucose concentration was measured by the glucose oxidase method. Thereafter, the rate constant for plasma glucose disappearance (K_{itt}) was calculated using the formula $0.693/(t_{1/2})$. The plasma glucose $t_{1/2}$ was calculated from the slope of the least squares analysis of the plasma glucose concentrations during the linear phase of decline [23].

Blood pressure measurement. A tail-cuff system (MKIV, Narco BioSystems, Austin, Tex., USA) combining a transducer or amplifier which provides output signals proportional to cuff pressure and amplified Korotkoff sounds was used to obtain blood pressure measurements in conscious rats. This indirect approach permits repeated measurements with a close correlation (correlation coefficient =0.975) compared to direct intra-arterial recording [24].

Vascular tissue preparation for morphological analysis. Rats were heparinized, deeply anaesthetized with pentobarbital sodium and killed with a lethal dose of lidocaine. Aortae were fixed with 4% paraformaldehyde in 0.1 mol/l phosphate buffer, pH 7.4, dehydrated in alcohol and xylol and routinely paraffin embedded. Step sections (5 μm) were stained with hematoxylin and eosin. At least five step sections of ascending, arch, thoracic and abdominal aorta were examined by light microscopy. Fragments were deparaffinized and routinely processed for electronmicroscopy. Ultrathin sections were stained with uranylacetate and lead citrate and examined with a ZEISS EM 10 electron microscope.

Statistical analysis. Experiments were always carried out by studying the groups of animals in parallel (2-month-old vs 12-month-old male Wistar rats and SHR vs age-matched WKY male rats). Data are means±SEM of absolute or percent values. For comparisons, unpaired Student's *t* test was used. The significance level was set at *p* value of less than 0.05.

Results

Animal characteristics. The 12-month-old rats were heavier than the control rats (2m: 137±12 g vs 12m: 432±13 g, $p<0.0001$) and had higher contents of fat mass in different sites (bilateral epididymal fat – 2m: 2.89±0.31 g vs 12m: 4.01±0.22 g, $n=10$ each, $p=0.0127$; bilateral perirenal fat – 2m: 2.17±0.05 g vs 12m: 2.77±0.03 g, $n=10$ each, $p<0.0001$; mesenteric fat – 2m: 3.26±0.30 g vs 12m: 5.03±0.41 g, $n=10$ each, $p=0.0026$; Table 1). The lengths of 2- and 12-month-old rats were 20±2 cm and 24±1 cm ($n=10$ each, $p=0.09$), respectively. The 12-month-old rats had higher plasma concentrations of total cholesterol and triglycerides than the 2-month-old rats. Fasting blood glucose and systolic blood pressure were similar in the two groups. Older animals were more insulin resistant than the young control rats, as expressed by their higher serum insulin concentrations (2m: 25±4 vs 12m: 41±6, $n=10$ each, $p<0.05$) and lower plasma glucose disappearance rates measured by the fifteen minute insulin tolerance test (K_{itt} 2m: 4.31±0.56%/min vs K_{itt} 12m: 2.34±0.38%/min, $n=10$ each, $p=0.004$).

Table 2 shows comparative data regarding SHR and WKY strains. As noticed, the SHR had a smaller body weight than the WKY rats (WKY: 369±10 g vs SHR: 315±8 g, $p<0.0001$). Consistent with previous

Table 1. Characteristics of obese middle-aged Wistar rats (12-month-old) and the young control rats (2-month-old)

Groups	Body weight (g)	Blood glucose (mg/dl)	Serum insulin (μU/ml)	Systolic blood pressure (mmHg)	K_{itt} (%/min)	Cholesterol (mg/dl)	Triglycerides (mg/dl)
2-month-old	137±12 (n=30)	123±5 (n=10)	25±4 (n=10)	114±2 (n=10)	4.31±0.56 (n=10)	32±7 (n=10)	49±11 (n=10)
12-month-old	432±13[a] (n=30)	118±9 (n=10)	41±6[b] (n=10)	112±3 (n=10)	2.34±0.38[c] (n=10)	91±15[c] (n=10)	108±21[b] (n=10)

Data are given as means ± SEM. p values of less than 0.05 were considered to be significantly different.
[a] $p<0.0001$ vs young controls; [b] $p<0.05$ vs young controls; [c] $p<0.01$ vs young controls

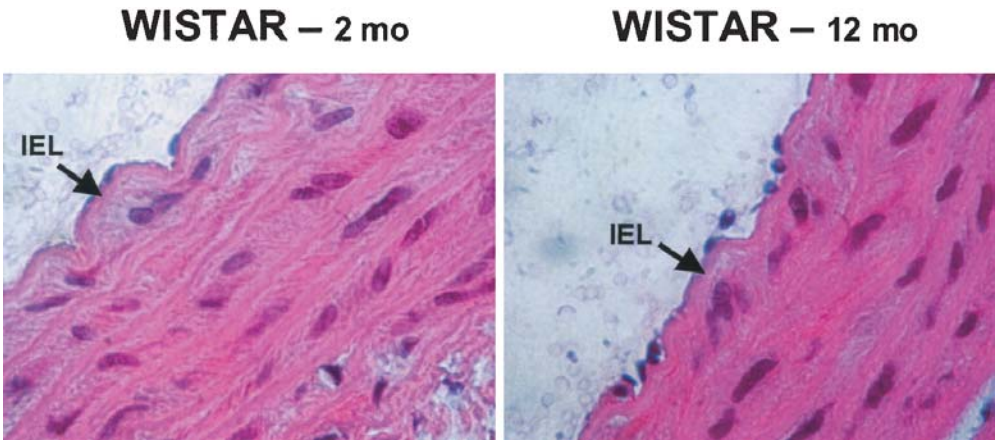

Fig. 1. Light photomicrographs of sections of HE stainings of thoracic aortae from 2- and 12-month-old Wistar rats. Magnification ×960. IEL=internal elastic lamina (*arrows*)

Table 2. Characteristics of SHR and the control rats, WKY

Groups	Body weight (g)	Blood glucose (mg/dl)	Serum insulin (μU/ml)	Systolic blood pressure (mmHg)	K_{itt} (%/min)	Cholesterol (mg/dl)	Triglycerides (mg/dl)
WKY	369±10 (*n*=30)	142±7 (*n*=10)	18±6 (*n*=10)	115±5 (*n*=10)	4.79±0.62 (*n*=10)	83±12 (*n*=10)	70±9 (*n*=10)
SHR	315±8[a] (*n*=30)	149±5 (*n*=10)	29±4 (*n*=10)	175±5[a] (*n*=10)	1.89±0.39[b] (*n*=10)	89±8 (*n*=10)	159±26[b] (*n*=10)

Data are given as means ± SEM. *p* values of less than 0.05 were considered to be significantly different.
[a] $p<0.0001$ vs WKY; [b] $p<0.01$ vs WKY

studies, systolic blood pressure was higher in SHR compared to the WKY rats (WKY: 115±5 mmHg vs SHR: 175±5 mmHg, $n=10$ each, $p<0.0001$). There were no differences between plasma concentrations of total cholesterol and glucose when the rats from these two strains were compared. Plasma concentration of triglycerides were higher in SHR than in WKY. SHR animals were more insulin resistant than the age-matched WKY as expressed by lower plasma glucose disappearance rates (K_{itt} WKY: 4.79±0.62%/min vs K_{itt} SHR: 1.89±0.39%/min, $n=10$ each, $p<0.01$) and higher, though not statistically significant, serum insulin concentrations.

Histological examination of aortae. In all step sections examined there were no signs of atherosclerotic changes, such as lipid and foam cell deposition, intimal thickening or SMC proliferation, neither on light microscopic examination (Fig. 1) nor on ultrastructural sections in aortae from the 12-month-old rats and the control rats.

Insulin signalling in skeletal muscle from 2-month-old and 12-month-old animals. There was no difference in insulin-stimulated tyrosine phosphorylation of insulin receptor beta subunit between muscles from 2- and 12-month-old rats (2m: 100±7% vs 12m: 100±4%, $n=6$; Fig. 2), and the protein concentrations of IRβ also did not change in obese middle-aged rats (Fig. 2B).

There was a greater decrease in insulin-stimulated IRS-1 tyrosine phosphorylation in muscles from obese, older rats than from the control rats (Fig. 2C, 2m: 100±5% vs 12m: 55±4%, $n=6$, $p<0.0001$). Also, IRS-1 protein concentrations were reduced in muscle from 12-month-old rats (2m: 100±9% vs 12m: 56±7%, $n=6$, $p<0.05$; Fig. 2D).

The insulin-stimulated association between IRS-1 and the p85 regulatory subunit of PI 3-kinase was also diminished in skeletal muscle from the 12-month-old rats compared to the 2-month-old control rats (2m: 100±5% vs 12m: 30±7%, $n=6$, $p<0.0001$; Fig. 2E).

Insulin was able to stimulate the serine phosphorylation of Akt in both groups of animals, but older animals showed a reduced concentration of Akt activation after insulin infusion (2m: 100±4% vs 12m: 41±3%, $n=6$, $p<0.0001$; Fig. 2F). The blot, representative of six experiments, was obtained after incubating the membranes with anti-Akt antibodies (Fig. 2G). There was no difference between the protein concentration of Akt in skeletal muscle from these two groups.

Insulin-stimulated Shc tyrosine phosphorylation in skeletal muscle from 12-month-old Wistar rats was not different from that observed in the 2-month-old group (Fig. 2H, $n=6$), without any difference in Shc protein expression between the two groups of animals (Fig. 2I).

Insulin was able to stimulate tyrosine phosphorylation of ERK1/2 equally in skeletal muscle from 2- and

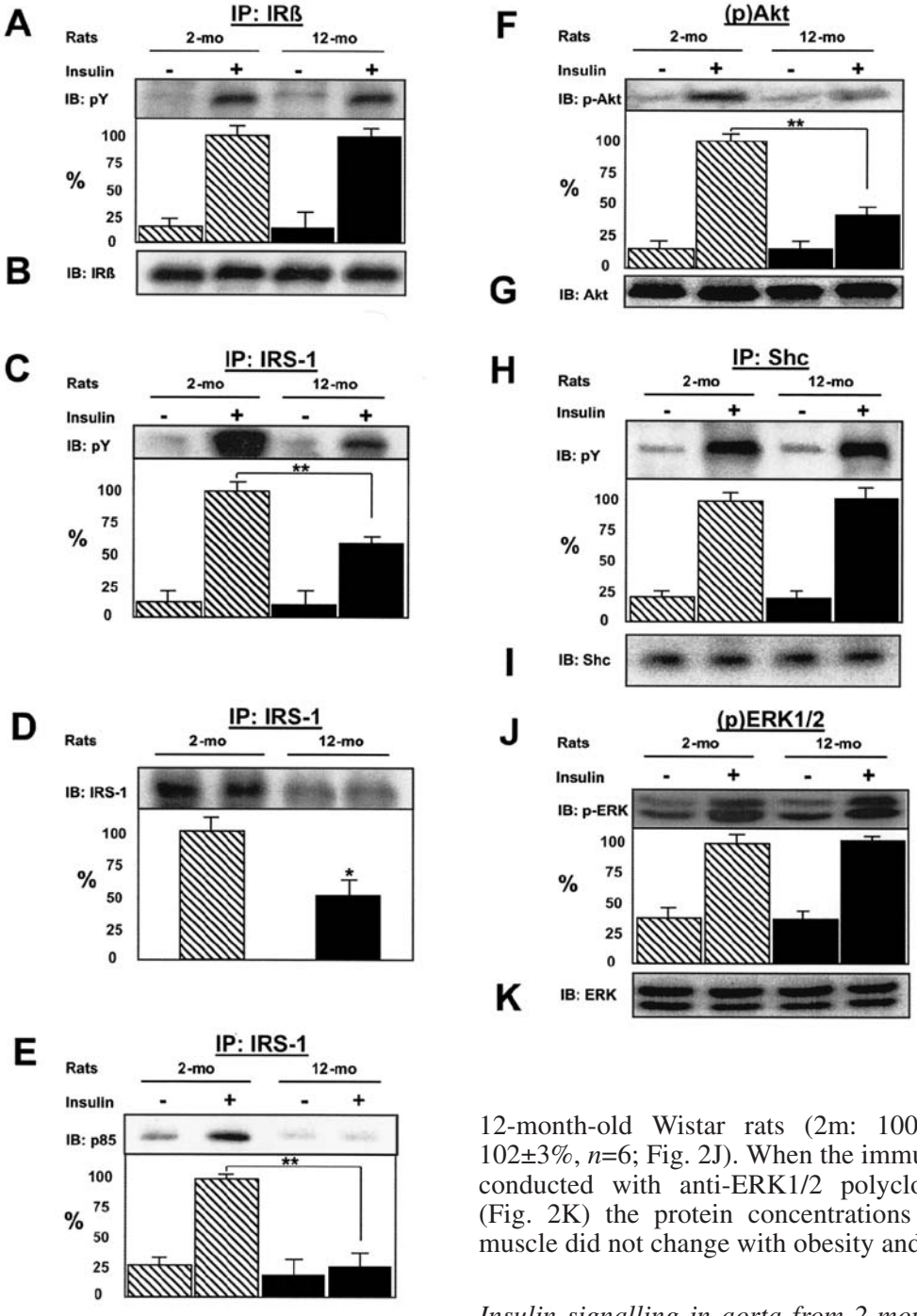

Fig. 2A–K. Insulin signalling in skeletal muscle of young (2-month-old) and middle-aged (12-month-old) Wistar rats. Insulin-stimulated insulin receptor tyrosine phosphorylation (**A**), insulin receptor protein concentrations (**B**), insulin-stimulated IRS-1 tyrosine phosphorylation (**C**), IRS-1 protein concentrations (**D**), insulin-stimulated association between IRS-1 and p85 (**E**), insulin-stimulated Akt serine phosphorylation (**F**), Akt protein concentrations (**G**), insulin-stimulated Shc tyrosine phosphorylation (**H**), Shc protein concentrations (**I**), insulin-stimulated ERK1/2 tyrosine phosphorylation (**J**) and ERK1/2 protein concentrations (**K**). Values are shown as the means ± SEM and are expressed as a percentage of the insulin-stimulated control (100%). *, $p<0.05$; **, $p<0.0001$

12-month-old Wistar rats (2m: 100±4% vs 12m: 102±3%, $n=6$; Fig. 2J). When the immunoblotting was conducted with anti-ERK1/2 polyclonal antibodies (Fig. 2K) the protein concentrations of ERK1/2 in muscle did not change with obesity and aging.

Insulin signalling in aorta from 2-month-old and 12-month-old animals. Insulin-stimulated IRβ tyrosine phosphorylation concentrations were similar in aortae from both young and middle-aged rats (representative of five different experiments, Fig. 3A). To evaluate the tissue levels of the insulin receptor beta subunit, nitrocellulose membranes of IRβ immunoprecipitates were stripped and reblotted with antibodies against IRβ (Fig. 3B). The tissue levels of IRβ did not change between the two groups.

There was no difference in insulin-stimulated IRS-1 tyrosine phosphorylation in aortae from 2- and 12-month-old rats (2m: 100±4% vs 12m: 105±3%, $n=6$; Fig. 3C). The same membranes were stripped and sub-

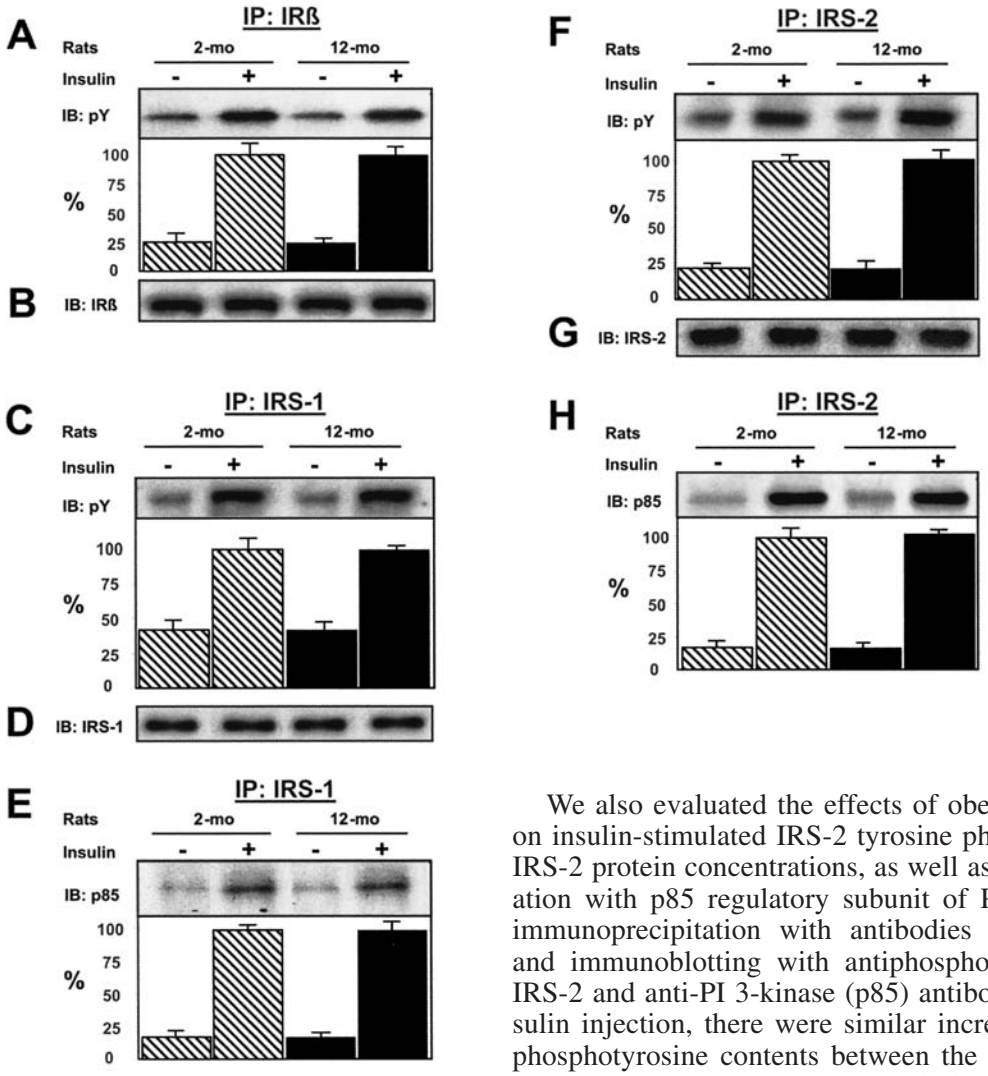

Fig. 3A–H. Insulin signalling in thoracic aortae of young (2-month-old) and middle-aged (12-month-old) Wistar rats. Insulin-stimulated insulin receptor tyrosine phosphorylation (**A**), insulin receptor protein concentrations (**B**), insulin-stimulated IRS-1 tyrosine phosphorylation (**C**), IRS-1 protein concentrations (**D**), insulin-stimulated association between IRS-1 and p85 (**E**), insulin-stimulated IRS-2 tyrosine phosphorylation (**F**), IRS-2 protein concentrations (**G**) and insulin-stimulated association between IRS-2 and p85 (**H**). Values are shown as the means ± SEM and are expressed as a percentage of the insulin-stimulated control (100%)

mitted to immunoblotting with anti-IRS-1 antibodies to evaluate the protein concentrations of IRS-1 in these tissues (Fig. 3D). No statistically significant difference was found in IRS-1 protein concentrations in the aortae of young and middle-aged rats.

The insulin-stimulated association between IRS-1 and the p85 regulatory subunit of PI 3-kinase in aorta was investigated (Fig. 3E). After stimulation with insulin, the association between IRS-1 and PI 3-kinase (p85) increased eightfold, with no difference between 2- and 12-month-old rats (2m: 100±5% vs 12m: 98±7%, n=6).

We also evaluated the effects of obesity and aging on insulin-stimulated IRS-2 tyrosine phosphorylation, IRS-2 protein concentrations, as well as IRS-2 association with p85 regulatory subunit of PI 3-kinase by immunoprecipitation with antibodies against IRS-2 and immunoblotting with antiphosphotyrosine, anti-IRS-2 and anti-PI 3-kinase (p85) antibodies. After insulin injection, there were similar increases in IRS-2 phosphotyrosine contents between the two groups of animals (2 m: 100±5% vs 12m: 95±6%, n=6; Fig. 3F). The tissue concentrations of IRS-2 were evaluated by immunoblotting with anti-IRS-2 antibodies, and showed no difference between the two groups of rats (Fig. 3G). Next, we evaluated the insulin-stimulated IRS-2 association with p85 subunit of PI 3-kinase in aortae from these animals (Fig. 3H). After insulin injection, p85 association to IRS-2 increased to 100±11% in 2-month-old rats and to 107±4% in 12-month-old rats (n=6 each, p=0.56), showing no significant difference between these two groups.

Basal concentrations of Akt serine phosphorylation in aorta were not different between the two groups of rats (2m: 53±10% vs 12m: 48±11%, n=10, p>0.05; Fig. 4A). Insulin was able to increase Akt serine phosphorylation in both groups of rats in a similar manner (2m: 100±6% vs 12m: 96±5%, n=10, p>0.05). When these membranes were submitted to immunoblotting with anti-Akt antibodies, as shown in (Fig. 4B) there was no difference between the two groups, indicating that vascular protein concentrations of Akt did not change with obesity and aging in Wistar male rats.

Akt is activated in response to insulin and so becomes capable of phosphorylating endothelial cell-

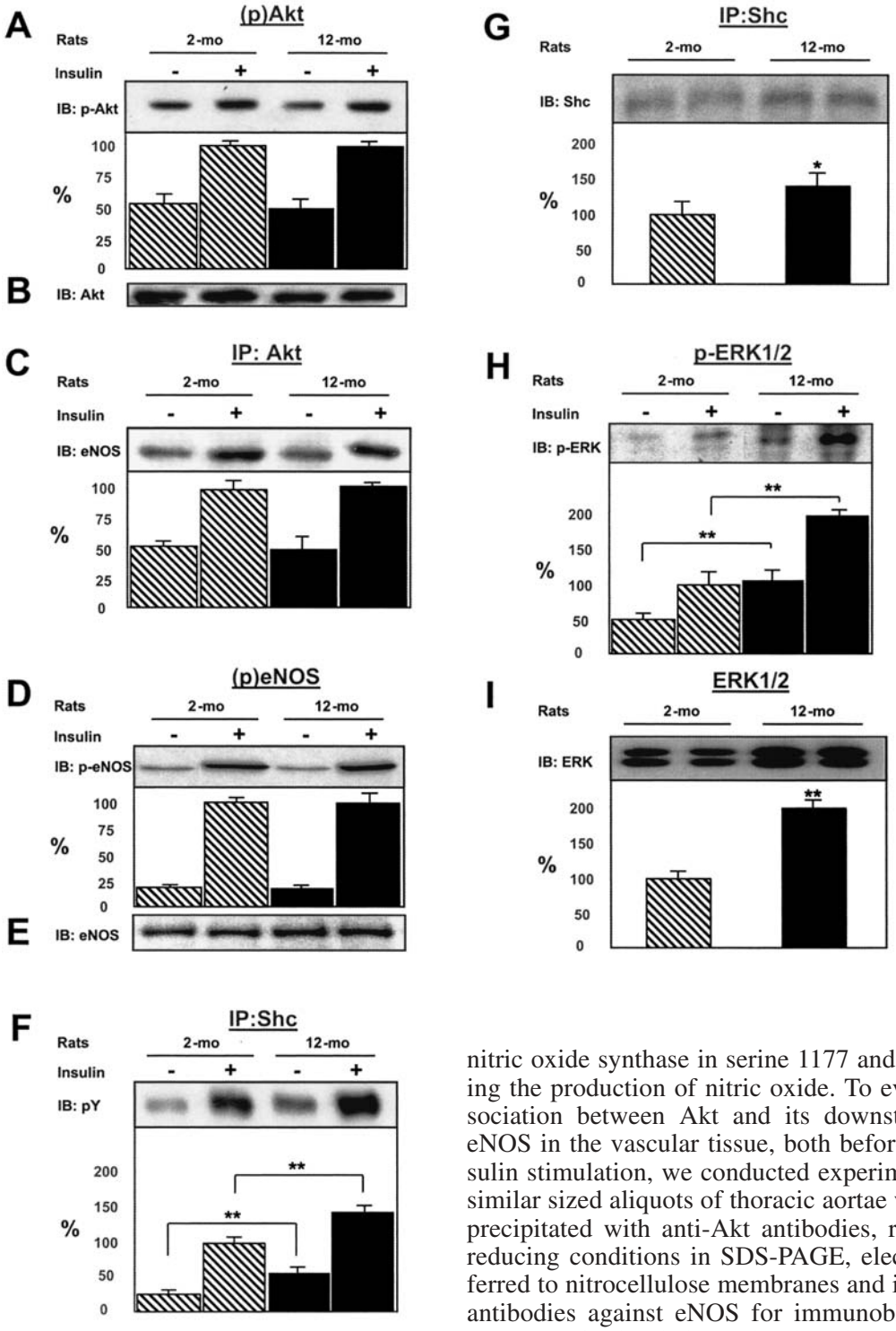

Fig. 4A–I. Insulin signalling in thoracic aortae of young (2-month-old) and middle-aged (12-month-old) Wistar rats. Insulin-stimulated Akt serine phosphorylation (**A**), Akt protein concentrations (**B**), insulin-stimulated association between Akt and eNOS (**C**), insulin-stimulated eNOS serine phosphorylation (**D**), eNOS protein concentrations (**E**), insulin-stimulated Shc tyrosine phosphorylation (**F**), Shc protein concentrations (**G**), insulin-stimulated ERK1/2 tyrosine phosphorylation (**H**) and ERK1/2 protein concentrations (**I**). Values are shown as the means ± SEM and are expressed as a percentage of the insulin-stimulated control (100%). *, $p<0.05$; **, $p<0.0001$

nitric oxide synthase in serine 1177 and 1179, activating the production of nitric oxide. To evaluate the association between Akt and its downstream effector eNOS in the vascular tissue, both before and after insulin stimulation, we conducted experiments in which similar sized aliquots of thoracic aortae were immunoprecipitated with anti-Akt antibodies, resolved under reducing conditions in SDS-PAGE, electrically transferred to nitrocellulose membranes and incubated with antibodies against eNOS for immunoblotting. In the absence of stimulation with insulin, the association between Akt and eNOS in aorta is discrete, represented by faint bands, and was not different between young and middle-aged rats (2m: 52±4% vs 12m: 50±8%, $n=6$, $p>0.5$; Fig. 4C). However, after stimulation with insulin, their association increased twofold, consistent with a stable association of Akt and eNOS, with no difference between 2- and 12-month-old rats (2m: 100±7% vs 12m: 104±3%, $n=6$, $p>0.5$).

Whole cell lysates obtained from thoracic aortae before or 3 min after insulin injection into the cava

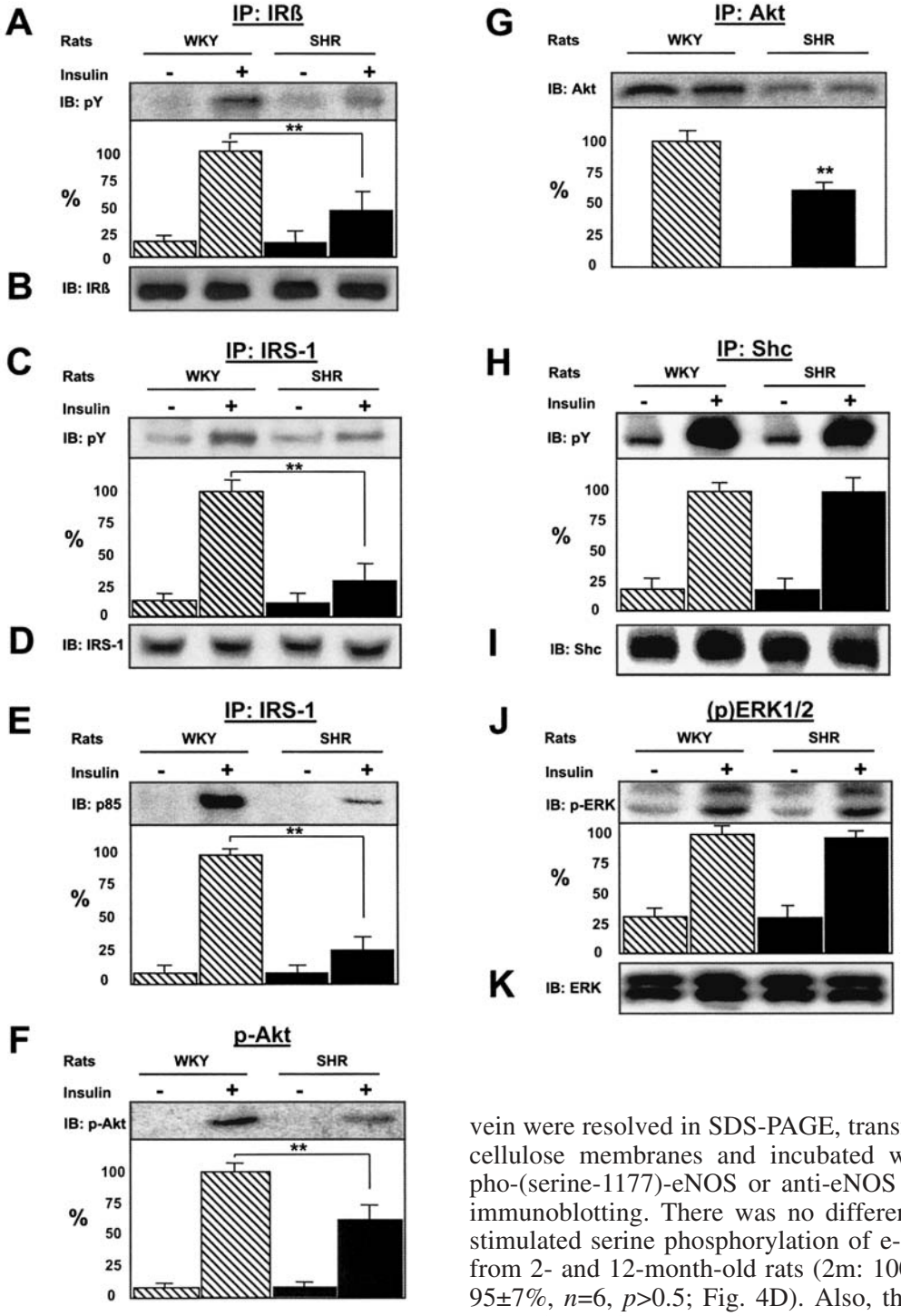

Fig. 5A–K. Insulin signalling in skeletal muscle of spontaneously hypertensive rats (SHR) and Wistar-Kyoto (WKY) rats. Insulin-stimulated insulin receptor tyrosine phosphorylation (**A**), insulin receptor protein concentrations (**B**), insulin-stimulated IRS-1 tyrosine phosphorylation (**C**), IRS-1 protein concentrations (**D**), insulin-stimulated association between IRS-1 and p85 (**E**), insulin-stimulated Akt serine phosphorylation (**F**), Akt protein concentrations (**G**), insulin-stimulated Shc tyrosine phosphorylation (**H**), Shc protein concentrations (**I**), insulin-stimulated ERK1/2 tyrosine phosphorylation (**J**) and ERK1/2 protein concentrations (**K**). Values are shown as the means ± SEM and are expressed as a percentage of the insulin-stimulated control (100%). $^{**}p<0.0001$

vein were resolved in SDS-PAGE, transferred to nitrocellulose membranes and incubated with anti-phospho-(serine-1177)-eNOS or anti-eNOS antibodies for immunoblotting. There was no difference in insulin-stimulated serine phosphorylation of e-NOS in aortae from 2- and 12-month-old rats (2m: 100±3% vs 12m: 95±7%, n=6, p>0.5; Fig. 4D). Also, the protein concentrations of e-NOS did not change between these two groups (Fig. 4E).

Both before and after stimulation with insulin, Shc showed higher degrees of tyrosine phosphorylation in aortae from 12-month-old Wistar rats as compared to the 2-month-old animals (without insulin: 2m: 28±4% vs 12m: 56±4%, n=6, p<0.0001; with insulin: 2m: 100±4% vs 12m: 145±4%, n=6, p<0.0001; Fig. 4F). This greater level of activation was accompanied by an increase in Shc protein concentrations in aortae from 12-month-old rats (2m: 100±8% vs 12m: 136±6%, n=6, p<0.05; Fig. 4G).

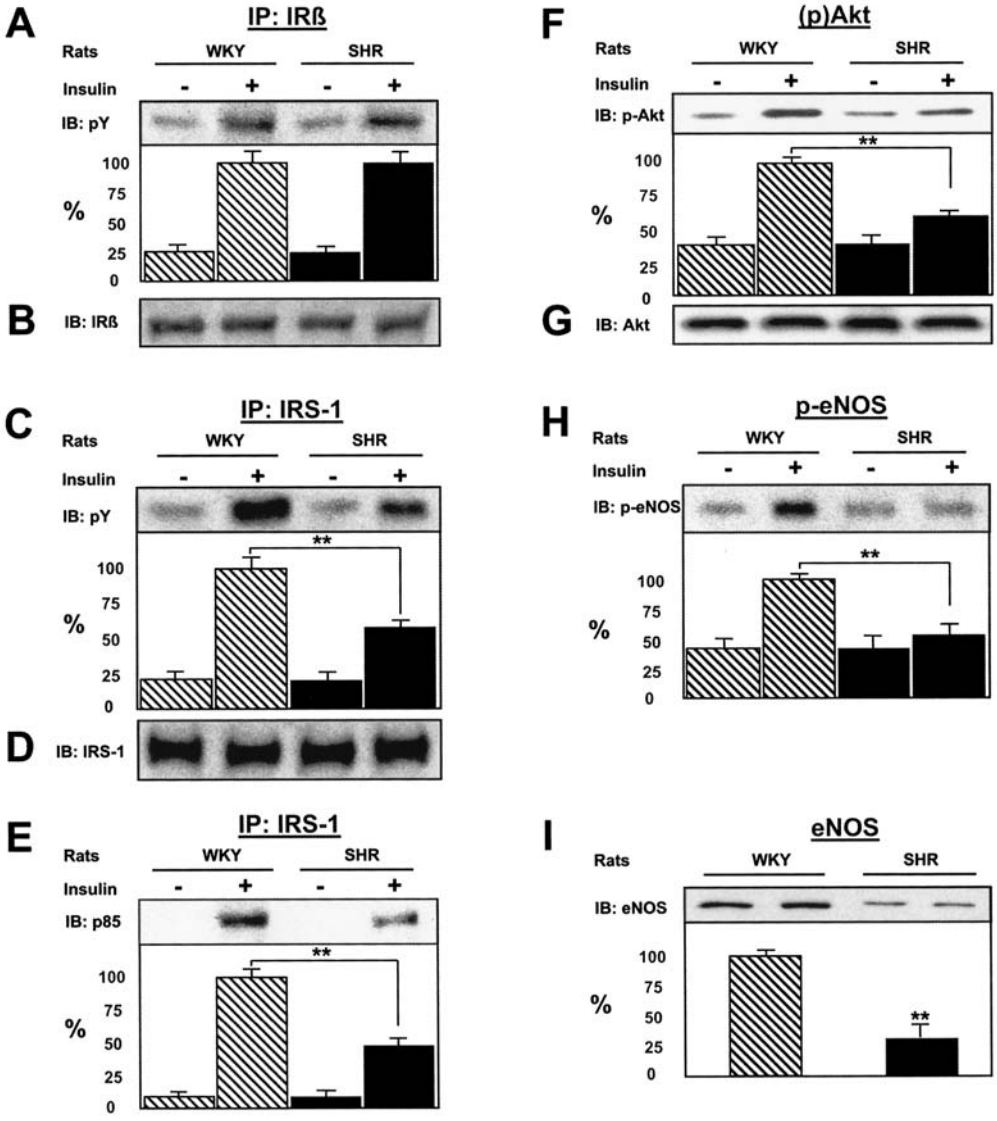

Fig. 6A–I. Insulin signalling in thoracic aortae of spontaneously hypertensive rats (SHR) and Wistar-Kyoto (WKY) rats. Insulin-stimulated insulin receptor tyrosine phosphorylation (**A**), insulin receptor protein concentrations (**B**), insulin-stimulated IRS-1 tyrosine phosphorylation (**C**), IRS-1 protein concentrations (**D**), insulin-stimulated association between IRS-1 and p85 (**E**), insulin-stimulated Akt serine phosphorylation (**F**), Akt protein concentrations (**G**), insulin-stimulated eNOS serine phosphorylation (**H**) and eNOS protein concentrations (**I**). Values are shown as the means ± SEM and are expressed as a percentage of the insulin-stimulated control (100%). $^{**}p<0.0001$

Using monoclonal antibodies against Tyr-204 phosphorylated ERK1 and ERK2, the levels of ERK1/2 activation were examined in rat thoracic aortae in the basal state and after insulin stimulation in the in vivo experiments. Insulin was able to stimulate tyrosine phosphorylation of ERK1/2 differentially in aortae from 2- and 12-month-old Wistar rats (Fig. 4H). Of note, 12-month-old rats showed increased basal tyrosine phosphorylation of ERK1/2, 2.2-fold higher than those found in young rats (2m: 50±5% vs 12m: 110±6%, n=12, $p<0.0001$). After insulin injection into the cava vein, tyrosine phosphorylation of ERK1/2 was two times higher in aortae from obese middle-aged rats than in the control rats (2m: 100±8% vs 12m: 208±4%, n=12, $p<0.0001$). Next, whole tissue extracts obtained from aortae homogenates from young and middle-aged rats were resolved under reducing conditions in 10% SDS-PAGE, transferred to nitrocellulose membranes and incubated with polyclonal antibodies against ERK1/2 proteins to evaluate the tissue levels of these protein kinases. Obese middle-aged rats demonstrated 2.1 times higher levels of ERK1/2 in aortae than the younger control rats (2m: 100±4% vs 12m: 210±8%, n=12, $p<0.0001$; Fig. 4I).

Insulin signalling in skeletal muscle from SHR and WKY

Insulin-stimulated tyrosine phosphorylation of insulin receptor beta subunit was reduced in skeletal muscle from SHR, as compared to the control rats (WKY: 100±3% vs SHR: 47±8%, n=9, $p<0.0001$; Fig. 5A). The protein concentrations of IRβ did not change in muscle samples obtained from SHR and WKY (Fig. 5B).

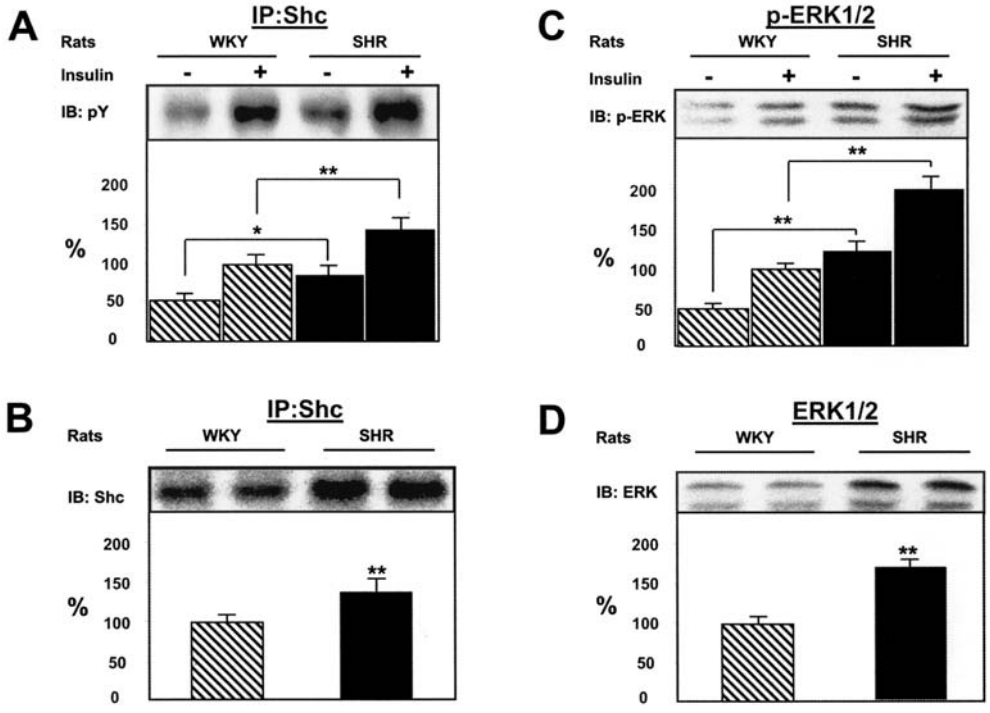

Fig.7A–D. Insulin signalling in thoracic aortae of spontaneously hypertensive rats (SHR) and Wistar-Kyoto (WKY) rats. Insulin-stimulated Shc tyrosine phosphorylation (**A**), Shc protein concentrations (**B**), insulin-stimulated ERK1/2 tyrosine phosphorylation (**C**) and ERK1/2 protein concentrations (**D**). Values are shown as the means ± SEM and are expressed as a percentage of the insulin-stimulated control (100%). *, $p<0.05$; **, $p<0.0001$

The insulin-stimulated IRS-1 tyrosine phosphorylation showed a decrease in skeletal muscle from SHR as compared to WKY (WKY: 100±6% vs SHR: 30±8%, n=9, $p<0.0001$; Fig. 5C). IRS-1 protein concentrations suffered no changes in muscle from these two groups (Fig. 5D). The insulin-stimulated association between IRS-1 and the p85 subunit of PI 3-kinase was also reduced in muscle from SHR as compared to WKY (WKY: 100±4% vs SHR: 26±8%, n=9, $p<0.0001$; Fig. 5E).

Insulin was able to stimulate the serine phosphorylation of Akt in skeletal muscle from WKY and SHR groups of animals, but the latter showed reduced Akt activation after insulin infusion (WKY: 100±4% vs SHR: 60±6%, n=9, $p<0.0001$; Fig. 5F). A parallel decrease in Akt protein expression in skeletal muscle from SHR in comparison to WKY strain was observed (WKY: 100±8% vs SHR: 62±4%, n=9, $p<0.0001$; Fig. 5G).

Insulin-stimulated Shc tyrosine phosphorylation in skeletal muscle from SHR was not different from that observed in the WKY group (representative of six experiments, Fig. 5H), with no difference in protein concentrations (Fig. 5I).

Insulin infusion stimulated the tyrosine phosphorylation of ERK1/2 equally in skeletal muscle from WKY and SHR (WKY: 100±5% vs SHR: 97±4%, n=6; Fig. 5J). The immunoblotting was then conducted with anti-ERK1/2 antibodies (Fig. 5K) to show that protein concentrations of ERK1/2 in muscle did not change between these two groups.

Insulin signalling in aorta from SHR and WKY Insulin-stimulated IRβ tyrosine phosphorylation concentrations were similar in aortae from both groups of animals (WKY: 100±6% vs SHR: 95±6%, n=9; Fig. 6A). There was no difference in tissue levels of IRβ when the two groups were compared (Fig. 6B).

There was a reduction in insulin-stimulated IRS-1 tyrosine phosphorylation in aortae from SHR when compared to WKY control rats (WKY: 100±6% vs SHR: 60±4%, n=9, $p<0.0001$; Fig. 6C). However, no differences were found in IRS-1 protein concentrations in the aortae of WKY and SHR (Fig. 6D).

After insulin injection, the association between IRS-1 and PI 3-kinase (p85) was decreased in aortae from SHR in comparison to WKY (WKY: 100±6% vs SHR: 48±4%, n=9, $p<0.0001$; Fig. 6E).

The insulin-stimulated Akt serine phosphorylation was reduced in aortae from SHR when compared to WKY (WKY: 100±4% vs SHR: 62±3%, n=9, $p<0.0001$; Fig. 6F). There was no difference between the Akt protein concentrations in aortae from these two strains (Fig. 6G).

There was a reduction in insulin-stimulated serine phosphorylation of e-NOS in aortae from SHR compared to the control rats (WKY: 100±3% vs SHR: 53±6%, n=9, $p<0.0001$; Fig. 6H). In addition, protein concentrations of the endothelial isoform of NOS

were also reduced in aortae from SHR (WKY: 100±4% vs SHR: 33±7%, n=9, p<0.0001; Fig. 6I).

The basal Shc tyrosine phosphorylation in aortae from SHR was higher than in the WKY control rats (WKY: 50±4% vs SHR: 73±4%, n=9, p<0.05; Fig. 7A). The increase in Shc tyrosine phosphorylation in the vascular tissue after acute insulin infusion was greater in SHR when compared to the WKY group (WKY: 100±6% vs SHR: 140±6%, n=9, p<0.0001; Fig. 7A). This increased level of Shc phosphorylation was accompanied by an increase in protein concentrations found in aortae from SHR (WKY: 100±3% vs SHR: 137±6%, n=9, p<0.0001; Fig. 7B).

The levels of ERK1/2 activation were then examined in the vascular tissue both in the basal state and after acute insulin stimulation. Insulin was able to stimulate tyrosine phosphorylation of ERK1/2 differentially in aortae from SHR and WKY groups (Fig. 7C). Basal tyrosine phosphorylation of these two isoforms of MAP kinase in aortae from SHR was higher than in the WKY control rats (WKY: 50±2% vs SHR: 121±3%, n=9, p<0.0001; Fig. 7C). After insulin injection, there was also a greater increase in ERK1/2 tyrosine phosphorylation in aortae from SHR when compared to the WKY group (WKY: 100±1% vs SHR: 200±5%, n=9, p<0.0001; Fig. 7C). To further analyse the protein concentrations of ERK1/2 in this tissue, membranes were submitted to immunoblot with anti-ERK1/2 antibodies. SHR showed 1.6 times higher levels of ERK1/2 in aortae than in the controls (WKY: 100±7% vs SHR: 167±3%, n=9, p<0.0001; Fig. 7D).

Discussion

Reduced insulin sensitivity has been proposed as an important risk factor in the development of endothelial dysfunction and atherosclerosis and is also associated with hypertension [25]. Vascular diseases represent an important cause of the morbidity and mortality associated with diabetes and other insulin resistant states. A very large body of experimental work has sought to elucidate the cellular and molecular mechanisms that underlie this important pathophysiological process. We have characterized insulin signal transduction pathways in the vasculature of young (2-month-old) and obese middle-aged (12-month-old) Wistar male rats and also in SHR and in their normotensive, insulin-sensitive control strain, WKY. The 12-month-old rats are obese and have insulin resistance, normal fasting blood glucose, increased serum insulin and insulin resistance, characterized by a reduced glucose disappearance rate during the insulin tolerance test, but they develop neither hypertension nor atherosclerosis. In contrast, the SHR is a model characterized by hypertension and insulin resistance [26, 27], and this alteration in insulin sensitivity was confirmed in our study by the reduced glucose disappearance rate during the ITT.

The molecular mechanism of insulin resistance in obese middle-aged animals is probably related to abnormalities in insulin signalling pathways in skeletal muscle. The PI 3-kinase/Akt pathway is severely impaired in skeletal muscle from these rats, with reductions in insulin-stimulated phosphorylation of IRS-1 and Akt, as well as IRS-1 protein concentrations and in the association between IRS-1/PI 3-kinase, as described previously [28]. Since activation of PI 3-kinase pathway by insulin is linked to metabolic functions such as glucose transport and glycogen and protein synthesis [29, 30, 31, 32], alterations in insulin signalling pathways in muscle can contribute to the insulin resistance observed in these animals. In contrast, tyrosine phosphorylation of IRβ and IRS-1/2, insulin-stimulated association between IRS-1/2 and PI 3-kinase, and serine phosphorylation of Akt and eNOS are preserved in their aortae. The molecular mechanism of this tissue-specific regulation of insulin signalling (reduced in muscle and preserved in aorta) in the obese insulin-resistant animals could be related to the expression of proteins involved in early steps of insulin action, to the level of serine phosphorylation of IRβ and IRSs and to the activity of phosphotyrosine phosphatases. On the other hand, in SHR there were reductions in IR/IRS-1/PI 3-K/Akt pathway in muscle and in IRS-1/PI 3-K/Akt/eNOS pathway in aorta, which could be involved in insulin resistance and could be one factor that can contribute to the endothelial dysfunction in these rats, respectively.

Recently, insulin signalling in vascular tissues has been emphasized. It has been shown that activation of PI 3-kinase pathway could be involved in insulin's stimulatory effect on NO release in cultured vascular endothelial cells [3]. This effect of insulin on NO could be responsible for insulin's vasodilatory actions and in some insulin-resistant states, the vasodilation induced by insulin could be blunted as a result of the inhibition of PI 3-kinase pathway [8, 9]. Furthermore, it has been shown that insulin-stimulated tyrosine phosphorylation of IRβ and IRS proteins and PI 3-kinase activation were selectively impaired in vascular tissues of insulin-resistant obese Zucker rats [33]. Also, it has been reported that insulin's vasodilatory effect could be partially due to increases in eNOS gene expression via PI 3-kinase pathway [6]. Accordingly, in vascular endothelial cell insulin receptor knockout mice there is a reduction in eNOS expression [34] suggesting that insulin resistance in vessels is accompanied by a reduction in this enzyme. From these reports and our results showing blunted insulin signalling through the IRS/PI 3-kinase/Akt/eNOS pathway associated with a reduction in eNOS expression in aortae from SHR, we can suggest that these alterations might contribute to the loss of insulin's effect on NO production, which could contribute to endothe-

lial dysfunction and could also play a role in the hypertension presented by SHR. In contrast, the obese middle-aged rats could be protected from cardiovascular disease, even if confronted by severe insulin resistance, because PI 3-kinase/Akt/eNOS pathway was preserved in aorta.

In contrast to PI 3-kinase activation, much less is known about insulin's activation of ERK1/2 MAP kinase in insulin-resistant or diabetic conditions in vivo. Selective hyperexpression of insulin signalling on ERK1/2 MAP kinase pathway in the vascular tissues could be pathophysiologically important in the development of cardiovascular diseases. Pathway-selective insulin resistance could result in increased potentiation of VSMC proliferation and production of plasminogen activator inhibitor-1 (PAI-1) via the Ras/Raf/MEK/MAP kinase pathway [33]. Activation of the MAP kinase pathway by insulin is not reduced in Type 2 diabetes, perhaps allowing for some of the detrimental effects of chronic hyperinsulinemia on cellular growth in the vasculature [35]. The increased expression and activation of Shc and ERK1/2 in aortae from SHR could suggest a role of this pathway in vascular abnormalities of this rat. However, in the obese middle-aged rat model of insulin resistance, the increased activation and protein concentrations of MAP kinase in aorta were not associated with SMC proliferation, as shown by histological results, neither with hypertension nor atherosclerosis. This suggests that the isolated activation of this pathway, with preservation of the PI 3-kinase/Akt/eNOS pathway, might not be sufficient for the development of cardiovascular diseases in these rats.

In summary, this study shows that alterations in IRS/PI 3-kinase/Akt pathway in muscle from 12-month-old rats and SHR could have a role in the insulin resistance of these rats. The preservation of this pathway in aorta of 12-month-old rats could be one factor that contributes to explaining the absence of cardiovascular disease in this animal model. However, in aortae of SHR, the reduced insulin signalling through IRS/PI 3-kinase/Akt/eNOS pathway could contribute to the endothelial dysfunction of this rat.

Acknowledgements. This work was supported by grants from Fundação de Amparo à Pesquisa do Estado de São Paulo (FAPESP). The authors would like to thank Mrs. E. Toth and Mr. L. Janieri for their technical assistance.

References

1. King GL, Goodman AD, Buzney S, Moses A, Kahn CR (1985) Receptors and growth-promoting effects of insulin and insulinlike growth factors on cells from bovine retinal capillaries and aorta. J Clin Invest 75:1028–1036
2. Obata T, Kashiwagi A, Maegawa H et al. (1996) Insulin signaling and its regulation of system A amino acid uptake in cultured rat vascular smooth muscle cells. Circ Res 79:1167–1176
3. Zeng G, Quon MJ (1996) Insulin-stimulated production of nitric oxide is inhibited by wortmannin. Direct measurement in vascular endothelial cells. J Clin Invest 98:894–898
4. Anderson PW, Zhang XY, Tian J et al. (1996) Insulin and angiotensin II are additive in stimulating TGF-beta 1 and matrix mRNAs in mesangial cells. Kidney Int 50:745–753
5. Tamaroglio TA, Lo CS (1994) Regulation of fibronectin by insulin-like growth factor-I in cultured rat thoracic aortic smooth muscle cells and glomerular mesangial cells. Exp Cell Res 215:338–346
6. Kuboki K, Jiang ZY, Takahara N et al. (2000) Regulation of endothelial constitutive nitric oxide synthase gene expression in endothelial cells and in vivo: a specific vascular action of insulin. Circulation 101:676–681
7. Papapetropoulos A, Rudic RD, Sessa WC (1999) Molecular control of nitric oxide synthases in the cardiovascular system. Cardiovasc Res 43:509–520
8. Scherrer U, Randin D, Vollenweider P, Vollenweider L, Nicod P (1994) Nitric oxide release accounts for insulin's vascular effects in humans. J Clin Invest 94:2511–2515
9. Steinberg HO, Brechtel G, Johnson A, Fineberg N, Baron AD (1994) Insulin-mediated skeletal muscle vasodilation is nitric oxide dependent. A novel action of insulin to increase nitric oxide release. J Clin Invest 94:1172–1179
10. Li H, Forstermann U (2000) Nitric oxide in the pathogenesis of vascular disease. J Pathol 190:244–254
11. Kasuga M, Karlsson FA, Kahn CR (1982) Insulin stimulates the phosphorylation of the 95,000-dalton subunit of its own receptor. Science 215:185–187
12. Sun XJ, Rothenberg P, Kahn CR et al. (1991) Structure of the insulin receptor substrate IRS-1 defines a unique signal transduction protein. Nature 352:73–77
13. Sun XJ, Wang LM, Zhang Y et al. (1995) Role of IRS-2 in insulin and cytokine signalling. Nature 377:173–177
14. Skolnik EY, Lee CH, Batzer A et al. (1993) The SH2/SH3 domain-containing protein GRB2 interacts with tyrosine-phosphorylated IRS1 and Shc: implications for insulin control of ras signalling. EMBO J 12:1929–1936
15. Myers MG Jr. Backer JM, Sun XJ et al. (1992) IRS-1 activates phosphatidylinositol 3′-kinase by associating with src homology 2 domains of p85. Proc Natl Acad Sci USA 89:10350–10354
16. Dimmeler S, Fleming I, Fisslthaler B, Hermann C, Busse R, Zeiher AM (1999) Activation of nitric oxide synthase in endothelial cells by Akt-dependent phosphorylation. Nature 399:601–605
17. Fulton D, Gratton JP, McCabe TJ et al. (1999) Regulation of endothelium-derived nitric oxide production by the protein kinase Akt. Nature 399:597–601
18. Trinder P (1969) Determination of blood glucose using an oxidase-peroxidase system with a non-carcinogenic chromogen. J Clin Pathol 22:158–161
19. Eizirik DL, Welsh N, Niemann A, Velloso LA, Malaisse WJ (1994) Succinic acid monomethyl ester protects rat pancreatic islet secretory potential against interleukin-1 beta (IL-1 beta) without affecting glutamate decarboxylase expression or nitric oxide production. FEBS Lett 337:298–302
20. Bradford MM (1976) A rapid and sensitive method for the quantitation of microgram quantities of protein utilizing the principle of protein-dye binding. Anal Biochem 72:248–254
21. Laemmli UK (1970) Cleavage of structural proteins during the assembly of the head of bacteriophage T4. Nature 227:680–685
22. Towbin H, Staehelin T, Gordon J (1979) Electrophoretic transfer of proteins from polyacrylamide gels to nitrocellulose sheets: procedure and some applications. Proc Natl Acad Sci USA 76:4350–4354

23. Bonora E, Moghetti P, Zancanaro C et al. (1989) Estimates of in vivo insulin action in man: comparison of insulin tolerance tests with euglycemic and hyperglycemic glucose clamp studies. J Clin Endocrinol Metab 68:374–378
24. Lovenberg W (1987) Techniques for the measurements of blood pressure. Hypertension 9 [Suppl]:15–16
25. Howard G, O'Leary DH, Zaccaro D et al. (1996) Insulin sensitivity and atherosclerosis. The Insulin Resistance Atherosclerosis Study (IRAS) Investigators. Circulation 93:1809–1817
26. Reaven GM (1991) Insulin resistance, hyperinsulinemia, hypertriglyceridemia, and hypertension. Parallels between human disease and rodent models. Diabetes Care 14:195–202
27. Mondon CE, Reaven GM (1988) Evidence of abnormalities of insulin metabolism in rats with spontaneous hypertension. Metabolism 37:303–305
28. Carvalho CR, Brenelli SL, Silva AC, Nunes AL, Velloso LA, Saad MJ (1996) Effect of aging on insulin receptor, insulin receptor substrate-1, and phosphatidylinositol 3-kinase in liver and muscle of rats. Endocrinology 137:151–159
29. Cheatham B, Vlahos CJ, Cheatham L, Wang L, Blenis J, Kahn CR (1994) Phosphatidylinositol 3-kinase activation is required for insulin stimulation of pp70 S6 kinase, DNA synthesis, and glucose transporter translocation. Mol Cell Biol 14:4902–4911
30. Haruta T, Morris AJ, Rose DW, Nelson JG, Mueckler M, Olefsky JM (1995) Insulin-stimulated GLUT4 translocation is mediated by a divergent intracellular signaling pathway. J Biol Chem 270:27991–27994
31. Mendez R, Myers MG, Jr., White MF, Rhoads RE (1996) Stimulation of protein synthesis, eukaryotic translation initiation factor 4E phosphorylation, and PHAS-I phosphorylation by insulin requires insulin receptor substrate 1 and phosphatidylinositol 3-kinase. Mol Cell Biol 16:2857–2864
32. Shepherd PR, Nave BT, Siddle K (1995) Insulin stimulation of glycogen synthesis and glycogen synthase activity is blocked by wortmannin and rapamycin in 3T3-L1 adipocytes: evidence for the involvement of phosphoinositide 3-kinase and p70 ribosomal protein-S6 kinase. Biochem J 305:25–28
33. Jiang ZY, Lin YW, Clemont A et al. (1999) Characterization of selective resistance to insulin signaling in the vasculature of obese Zucker (fa/fa) rats. J Clin Invest 104:447–457
34. Kondo T, Vincent D, Ilany J, King GL, Kahn CR (2002) Roles of insulin receptors in endothelial cells in metabolism and proliferative retinopathy. Diabetes 51 [Suppl 2]: A80 (Abstract)
35. Cusi K, Maezono K, Osman A et al. (2000) Insulin resistance differentially affects the PI 3-kinase- and MAP kinase-mediated signaling in human muscle. J Clin Invest 105:311–320